



**HAL**  
open science

## The role of membrane physiology in sHSP Lo18-lipid interaction and lipochaperone activity

Tiffany Bellanger, Frank Wien, Sophie Combet, Paloma Fernández Varela,  
Stéphanie Weidmann

► **To cite this version:**

Tiffany Bellanger, Frank Wien, Sophie Combet, Paloma Fernández Varela, Stéphanie Weidmann. The role of membrane physiology in sHSP Lo18-lipid interaction and lipochaperone activity. Scientific Reports, 2024, 14 (1), pp.17048. 10.1038/s41598-024-67362-6 . hal-04797845

**HAL Id: hal-04797845**

**<https://hal.science/hal-04797845v1>**

Submitted on 22 Nov 2024

**HAL** is a multi-disciplinary open access archive for the deposit and dissemination of scientific research documents, whether they are published or not. The documents may come from teaching and research institutions in France or abroad, or from public or private research centers.

L'archive ouverte pluridisciplinaire **HAL**, est destinée au dépôt et à la diffusion de documents scientifiques de niveau recherche, publiés ou non, émanant des établissements d'enseignement et de recherche français ou étrangers, des laboratoires publics ou privés.

# 1 The role of membrane physiology in sHSP Lo18 -lipid interaction and lipochaperone activity

## 2 Short Title: Lo18 membrane activity affected by lipid profiles

3  
4 **Tiffany Bellanger<sup>a</sup>, Frank Wien<sup>b</sup>, Sophie Combet<sup>c</sup>, Paloma Fernández Varela<sup>d</sup>, Stéphanie Weidmann<sup>a#</sup>**

6 <sup>a</sup> Procédés Alimentaires et Microbiologiques (PAM), AgroSup Dijon, PAM UMR A 02.102, Laboratoire  
7 VALMiS-IUVV, Dijon, France.

8 # Correspondence: stephanie.desroche@u-bourgogne.fr

9 <sup>b</sup>: Synchrotron SOLEIL, L'Orme des Merisiers, Saint Aubin BP 48, 91192, Gif-sur-Yvette, France

10 <sup>c</sup>: Laboratoire Léon-Brillouin (LLB), UMR12 CEA, CNRS, Université Paris-Saclay, F-91191, Gif-sur-Yvette  
11 CEDEX, France

12 <sup>d</sup>: Université Paris-Saclay, CEA, CNRS, Institute for Integrative Biology of the Cell (I2BC), 91198 Gif-sur-  
13 Yvette, France

### 14 15 **Abstract**

16 Lactic acid bacteria, such as *O. oeni*, face stress that affects membrane fluidity. To overcome  
17 this, small HSP are produced and act as chaperones and lipochaperones. However, the  
18 molecular mechanisms involved in lipochaperone activity are still poorly understood, particularly  
19 with regard to the influence of membrane lipid composition on this activity. This work aimed at  
20 characterizing the influence of the lipid environment and the physiological state of the membrane  
21 on the structure and lipochaperone activity of Lo18. In this context, liposomes derived from *O.*  
22 *oeni* cultures in exponential, stationary and adapted growth phases at 8% alcohol, representing  
23 the physiological states of unstressed, stressed and stress-adapted bacterial membranes, were  
24 produced and characterized. These liposomes were then used to observe the effect of the  
25 physiological state of the membranes on the lipochaperone activity and structural changes of  
26 Lo18. The results allowed us to identify the preferential affinity of Lo18 for lipids composed of  
27 oleic acid and/or phosphatidylglycerol, the mainly phospholipid component of the membranes  
28 not yet adapted to stress. The impact of this membrane composition on the structure,  
29 lipochaperone activity and the insertion of Lo18 into the different types of liposomes showed that:  
30 (i) the presence of the membrane (regardless of its nature) induces a modification of the structure  
31 of Lo18; (ii) the insertion of Lo18 into the membrane and/or the lipochaperone activity of Lo18 is  
32 enhanced when the membranes are rich in oleic acid and/or phosphatidylglycerol. This work  
33 contributes to a better understanding of interaction mechanisms between sHSPs and bacterial  
34 membranes.

### 35 36 **Introduction**

37  
38 The acidity and alcohol concentration present in wine are the main causes of membrane damage  
39 found in wine-grown cells [1]. Changes in the charge environment induced by low pH or -OH  
40 residues, which have a strong affinity for the polar heads of phospholipids, disrupt the  
41 organization and structure of the membrane, which has an impact on cell permeability and  
42 membrane fluidity [2, 3]. However, maintaining membrane fluidity is essential for the survival of

43 micro-organisms. Any change in membrane fluidity disrupts the flux of nutrients/wastes across  
44 the membrane and dissipates the proton motive force [4, 5], which can slow down cell  
45 metabolism, leading to cell growth arrest [6, 7]. Most of the key micro-organisms involved in the  
46 winemaking process have developed different strategies to maintain their membrane integrity.

47

48 For *Oenococcus oeni*, the main lactic acid bacteria involved in malolactic fermentation, one of  
49 these mechanisms is the synthesis of stress proteins, such as its unique small heat shock protein  
50 (sHSP) named Lo18. sHSPs are small proteins of 12 to 42 kDa, present in almost all organisms.  
51 In oligomeric state, they are mainly known for their ability to prevent the aggregation of cellular  
52 proteins owing to their chaperone activity [8–11]. However, for some sHSPs a second activity,  
53 known as molecular lipochaperone, has been described consisting in helping cells to maintain  
54 optimal membrane fluidity. Among these sHSPs are: HSPB1 and HSPB5 from humans [12], HSPA  
55 from *Synechococcus sp.* [10, 13], HSP17 from *Synechocystis sp.* [14, 15], HSP17.8 from  
56 *Arabidopsis thaliana* [16], HSP15.8 and HSP16 from *Schizosaccharomyces pombe* [17],  
57 HSP18.55 from *Lactiplantibacillus plantarum* [18] and Lo18 [11, 19–24]. According to the  
58 literature, when oligomers dissociate into dimers close to the membrane, electrostatic and  
59 hydrophobic forces deform the protein, allowing it to partially penetrate into the membrane and  
60 maintain optimal fluidity [25]. Regarding Lo18, previous studies have shown: (i) that the structure  
61 and oligomeric plasticity of the protein have an impact on lipochaperone activity [23, 24], and (ii)  
62 that Lo18 preferentially interacts with membrane lipids not yet adapted to stress [23]. However,  
63 the link between Lo18 lipochaperone activity, and more generally sHSPs, and the membrane lipid  
64 profile remains poorly described and understood.

65

66 The main aim of this study was to elucidate the links between the lipochaperone activity of Lo18  
67 and the lipid composition and physical state of the membranes with which it interacts. First, the  
68 affinity of Lo18 for certain phospholipids constituting the membranes of *O. oeni* was investigated  
69 by immunolabelling, revealing a significant preference for lipids composed of  
70 phosphatidylglycerol and/or oleic acid. In parallel, the lipochaperone activity and structural  
71 changes of Lo18 were assessed during interaction with four types of liposomes representing the  
72 physiological states of unstressed, stressed and stress-adapted bacterial membranes. To do  
73 this, bacterial membranes from *O. oeni* from (i) exponential and stationary growth phase culture  
74 and (ii) 8% ethanol adapted culture were collected to create liposomes. The results showed that  
75 membrane interaction induced a change in the secondary structure of Lo18, characterized by an  
76 increase in  $\alpha$ -helices at the expense of  $\beta$ -sheets for the liposomes tested. Additionally, the lipid  
77 composition of liposomes could influence the insertion of Lo18 into the membrane and  
78 lipochaperone activity.

79

## 80 **Results**

81

### **Favored lipidic Lo18 substrates**

82 Over the last decade, a growing number of studies have focused on the lipochaperone activity of  
83 Lo18 [11, 20, 23, 24, 26]. However, to date, the lipid domains or lipids specifically involved in this  
84 interaction have not been identified. The affinity between Lo18 and several common  
85 phospholipids was analyzed by immunolabeling. The phospholipids were chosen for their  
86 presence in *O. oeni* membranes, and their physical properties. Regarding the physical properties,  
87 phospholipids were composed of: (i) either unsaturated (dioleoyl, DO-) or saturated (dipalmitoyl,

88 DP-) fatty acids, and (ii) neutral (phosphatidylethanolamine, -PE and phosphatidylcholine, -PC)  
89 or negative-charge head groups (phosphatidic acid, -PA and phosphatidylglycerol, -PG). The  
90 intensity of the signal obtained after hybridization with Lo18 was normalized with the quantity of  
91 phospholipids fixed on the PolyVinylidene Fluoride (PVDF) membrane (obtained after staining  
92 with Nile Red) (Supplementary Data, Fig. S1). After this normalization step, Lo18 showed  
93 increased affinity for oleic acid (DOPG, DOPC and DOPE) and/or with the phosphatidylglycerol  
94 head group (DPPG and DOPG) (Fig. 1). The unsaturation present in the carbon chains of oleic acid  
95 naturally induces a certain disorder in the membrane, which is often observed in membranes not  
96 yet adapted to fluidifying stresses [27]. As described for HSP16 from *S. pombe* [17] and human  
97 HSPB1 [12, 28], this suggest Lo18 may preferentially interact with lipids found at the beginning of  
98 fluidification due to both hydrophobic and electrostatic interaction forces.

99

100

### **Lipid membrane composition impacts Lo18 lipochaperone activity**

101 Given the affinity of Lo18 for certain phospholipids, it therefore seemed reasonable to examine  
102 whether the lipid composition and physiological state of membranes could have an impact on  
103 the lipochaperone activity of Lo18. To investigate this point, we used liposomes composed of  
104 purified lipids from cultures of *O. oeni* at different growth phases (exponential, stationary, and  
105 grown in the presence of 8% ethanol) representing the physiological states of unstressed,  
106 stressed and stress-adapted bacterial membranes, respectively. Liposomes composed of  
107 purified lipids from exponential *L. plantarum* cultures were also used as controls to test the  
108 specificity of Lo18 for lipids from its producer organism. The lipid composition of these four types  
109 of liposomes was first determined by chromatography (Fig. 2, Table S1). The results showed that  
110 digalactosyldiacylglycerols (DGDG) were the main head group found in *O. oeni* regardless of the  
111 growth phase, representing 38%, 64%, and 57% of the total head groups in liposomes from  
112 cultures in the exponential and stationary phases, or in the presence of 8% ethanol, respectively.  
113 For liposomes derived from the exponential phase culture of *O. oeni* and *L. plantarum*,  
114 phosphatidylglycerol (PG) represented a predominant head group, accounting for 39% of total  
115 lipids for *O. oeni* and 67% for *L. plantarum* (Fig. 1A, Table S1). Lysyl-PG, cardiolipins (CL) and  
116 phosphatidylcholins (PC) were also present in *O. oeni* and *L. plantarum* membranes in very low  
117 quantities, which could be considered as negligible. Regarding the fatty acid chains, they ranged  
118 from myristic acid, C14:0, to lactobacillic and dihydrosterulic acid (respectively cycC19:0 n-7 and  
119 cycC19:0 n-9), abbreviated C19:1 (Fig. 2B, Table S1). Palmitic acid, C16:0 (saturated), and oleic  
120 acid, C18:1 (unsaturated), were the most abundant fatty acids in *O. oeni* cells in the exponential  
121 and stationary phases in contrast with those present in *L. plantarum* cells, representing 37% and  
122 26% in the exponential phase, 29% and 25% in the stationary phase, and 42% and 20% for the *L.*  
123 *plantarum* membrane respectively. During adaptation to alcohol the proportion of unsaturated  
124 fatty acids was significantly reduced, representing 12% of lipids compared with 28% and 29% in  
125 the exponential and stationary phases. This was mainly due to the decrease in the proportion of  
126 C18:1, from 26% in the exponential and 25% in the stationary phases to 11% in the presence of  
127 ethanol adapted membrane. Thus, by examining the nature of the polar heads and the fatty acid  
128 chains, four distinct profiles based on the prevalence of phosphatidylglycerol and oleic acid  
129 could be distinguished. It should be recalled that they are among the preferred lipid substrates of  
130 Lo18. Liposomes derived from *O. oeni* cultures in the exponential growth-phase are rich in PG  
131 and oleic acid (PG+, DO+), while those from the stationary phase are low in PG but rich in oleic  
132 acid (PG-, DO+). Liposomes derived from alcohol-adapted cultures were low in PG and oleic acid

133 (PG-, DO-), while those derived from a *L. plantarum* culture were high in PG but low in oleic acid  
134 (PG+, DO-).

135 The variation of the membrane fluidity of these four liposomes was then measured by steady-  
136 state fluorescence anisotropy of a 1,6-diphenyl-1,3,5-hexatriene probe (DPH) in the absence or  
137 presence of Lo18 during thermal ramping from 15 °C to 65 °C (Fig. 3, Table S2). The higher  
138 anisotropy means lower membrane fluidity. The ability of the Lo18 protein to maintain membrane  
139 fluidity was specific to the physiological state of the cells used to produce liposomes. Indeed,  
140 Lo18 maintained the membrane fluidity in liposomes from exponential growth phase cultures of  
141 both *O. oeni* and *L. plantarum*. From 45°C, fluidity reached 68% and 62% of their initial anisotropy  
142 value, respectively, in the presence of Lo18 versus 52%, and 56% in the absence of Lo18.  
143 Regarding liposomes from *O. oeni* culture in the stationary phase, the lipochaperone activity of  
144 Lo18 appeared later at 65°C. Finally, the lipochaperone activity of Lo18 over liposomes from  
145 ethanol-adapted *O. oeni* cultures was completely abolished in the temperature range 15°C to  
146 65°C, where no difference was observed in the presence or absence of Lo18. However, it is  
147 important to take into account the difference in initial anisotropy, which is dependent on the lipid  
148 composition of the membranes used, and which may influence fluidization. This is particularly  
149 the case for membranes adapted to stress, which are more rigid.

#### 150 **Impact of membrane lipid composition on the secondary structure of Lo18**

151 The modification of Lo18 lipochaperone activity linked to the physiological state of the membrane  
152 used was further characterized by investigating the modification of Lo18 secondary structures.  
153 To do this, Synchrotron radiation circular dichroism (SRCD) experiments were performed on Lo18  
154 alone or in interaction with the four types of liposomes during thermal ramping from 20 °C to 60  
155 °C. Along this ramp, 45° C, the temperature (Fig. 4A) corresponding to the temperature at which  
156 Lo18 starts its lipochaperone activity, is particularly interesting and will therefore be described in  
157 detail. At 45°C, the proportion of  $\alpha$ -helices increases significantly when Lo18 interacts with  
158 liposomes, starting at 3% for the protein alone to 6%, 8%, 24% and 6% in the presence of  
159 liposomes from *O. oeni* cells in the exponential and stationary phases, and ethanol-adapted  
160 cultures, respectively, as well as with *L. plantarum* cells (Figure 4). In contrast, the interaction  
161 with liposomes decreases the proportion of  $\beta$ -sheets. For Lo18 alone, the proportion of  $\beta$ -sheets  
162 was 42%, compared to 37%, 35%, 21%, and 31% upon interaction with liposomes from the  
163 exponential and stationary phases, the alcohol-adapted culture of *O. oeni*, and the culture of *L.*  
164 *plantarum*, respectively (Fig. 4). Thus, the presence of lipids modifies the structure of Lo18 more  
165 significantly than lipid composition.

166 In addition, the insertion of Lo18 into the different types of liposomes was also monitored by  
167 SRCD. This insertion was highlighted by a shift in the spectrum of polarized light towards the lower  
168 frequencies (bathochromic effect) when Lo18 was in the presence of certain liposomes. A clearly  
169 visualized shoulder (Fig 4B, in a rectangle box) appeared in the 195-210 nm range with liposomes  
170 derived from *O. oeni* cells in the exponential and stationary phases between 15 °C to 45°C. For  
171 example, at 15°C, the  $\Delta\epsilon$  value at 200 nm was -10.1 and -11.6 for these liposomes, respectively,  
172 compared to -14.7 for the protein alone. This shoulder was totally absent in the two  
173 other conditions (-15.7 and -15.8 for liposomes derived from an alcohol-adapted culture and from  
174 a *L. plantarum* culture, respectively). Both these latter liposomes were the poorest in proportions  
175 of oleic acid in contrast to the liposomes from culture of *O. oeni* in exponential and stationary  
176 growth phases (Fig. 2). These differences in membrane composition, in particular the degree of  
177 fatty acid unsaturation, could influence membrane fluidity and also the distribution of

178 hydrophobic zones on the membrane surface. As Lo18 insertion is mainly observed in liposomes  
179 rich in oleic acid, it appears that this insertion can take place via hydrophobic interactions with  
180 relatively fluid membranes. The insertion could be observed up to 45°C (Fig. 4C), above which the  
181 structural change in Lo18 no longer allowed distinguishing this shoulder.

182

## 183 Discussion

184

185 Membranes are the first cellular component affected by environmental changes. The viscosity of  
186 the membrane must remain close to 0.1 Pa.s. However, as a function of time and the intensity of  
187 the stresses encountered, this viscosity will be modified, leading the cells to adapt by fluidizing  
188 or rigidifying their membrane. [29]. To maintain optimum membrane fluidity, cells deploy a variety  
189 of mechanisms. In bacteria, adjustments such as changes in (i) saturated/unsaturated fatty acid  
190 ratios, (ii) the nature of unsaturation, (iii) the length of fatty acid carbon chains, or (iv) changes in  
191 polar heads are frequently observed [29–32]. However, these response mechanisms can only  
192 regulate membrane fluidity in the long term. To cope rapidly with an alteration in membrane  
193 integrity, cells have the capacity to synthesize proteins that regulate membrane fluidity, like  
194 sHSPs Lo18 synthesized by *O. oeni* [11, 20, 21, 23, 24].

195 Previous studies have shown that Lo18 has a stronger affinity for lipid substrates than for protein  
196 substrates; especially when the lipid composition of membranes is not yet adapted to stress.  
197 Until now, no specific affinities with phospholipids has been identified.[23]. In this context, the  
198 affinity between Lo18 and several phospholipids chosen for their physical properties was  
199 determined by immunolabeling. Although Lo18 interacts specifically with all the phospholipids  
200 tested, its affinity is most pronounced for lipids with a polar head group of PG and/ or oleic acid  
201 fatty acid chains. No interaction with DOPA was evidenced, certainly due to its conical  
202 conformation that might be less accessible [33]. Due to physical properties of PG and oleic acid,  
203 i.e. negatively charged and unsaturated fatty acids, respectively, the results suggest that Lo18  
204 interacts via electrostatic and hydrophobic forces. These lipids are particularly represented in  
205 fluid membranes, classically found before lipid modification during adaptation to stress [29, 32,  
206 34–36]. Indeed, both of these two phospholipid constituents are predominant in the membranes  
207 of both the exponential phase cultures (from *O. oeni* et *L. plantarum*) tested, mimicking  
208 unstressed membranes. This specific affinity for negatively charged lipids or fluid membranes  
209 has been reported for other sHSPs, such as human HSPB1 [12, 28], HSP16 from *S. pombe* [17],  
210 HSP17 from *Synechocystis* [37] and HSP12 from *Ustilago maydis* [38]. In all these cases,  
211 interaction appears to be mediated both by the state of fluidity of the membrane and by charges  
212 present at the lipid head and certain domains of the sHSP [12, 28]. More precisely, the  
213 hydrophobic domain of fatty acids could be used as an anchoring surface [28] and negative  
214 charges could attract the sHSPs on this surface.

215 To test the impact of these unsaturated (oleic acid) and negatively charged (PG) domains on  
216 Lo18/membrane interaction, Lo18 insertion into liposomes containing lipids from *O. oeni* or *L.*  
217 *plantarum* cultures at different physiological states (exponential growth, stationary phase or  
218 adaptation to 8% ethanol) was monitored by SRCD. The PG and oleic acid concentrations of these  
219 liposomes varied: rich in PG and oleic acid for membranes from *O. oeni* cultures in exponential  
220 phase, poor in PG and rich in oleic acid for those in stationary phase, poor in PG and oleic acid for  
221 those adapted to alcohol, and rich in PG but poor in oleic acid for membranes from *L. plantarum*

222 cultures in exponential phase (Figure 5A). A loss of negative absorption and a batho-chromic (red-  
223 ) shift of the  $\pi$ - $\pi^*$  electronic transition at 208 nm translating protein insertion inability [39], were  
224 observed on SRCD spectra in the presence of ethanol-adapted liposomes and *L. plantarum*  
225 liposomes. Both these liposomes have the lowest content of oleic acids among the liposomes  
226 tested. This difference in fluidity mainly caused by the nature of the fatty acid chains, could  
227 change the insertion of Lo18 into the membrane as was observed for membrane proteins, human  
228 sHSPs such as HSPB1 and HSPB5 or HSP17 from *Synechocystis*, which insert more efficiently  
229 into liquid crystalline phase membranes than into gel phase membranes [12, 28, 38, 40–42].  
230 Indeed, the more rigid the membrane, the less mobile and more ordered the phospholipids are,  
231 thereby reducing the efficiency of protein insertion [32]. The decrease of protein insertion due to  
232 greater bilayer stability may have an impact on protein activity, particularly lipochaperone  
233 activity, without necessarily abolishing it [43].

234 In addition to the impact on Lo18 insertion, the lipid composition of membrane could also impact  
235 the structure of the protein [43]. Indeed, a modification in membrane fluidity caused by the  
236 modification of the ratio between saturated/unsaturated fatty acids may also modify the  
237 attractive force around the membrane, leading to a modification of the secondary structure of  
238 Lo18. The secondary structure of Lo18 was determined during Lo18-liposome interaction by  
239 SRCD measurement. After interaction with the four types of liposomes at 45°C, an increase in the  
240 proportion of  $\alpha$ -helices to the detriment of  $\beta$ -sheets was observed compared to the Lo18 protein  
241 alone. However, as this structural change occurred to a greater or lesser extent for all the  
242 liposomes tested, the presence of lipids (rather than their nature) was sufficient to cause the  
243 structural change in Lo18 [26, 44].

244

245 Both insertion and secondary structure modification due to membrane lipid composition may  
246 contribute to Lo18 lipochaperone activity [26]. Consequently, Lo18 lipochaperone activity was  
247 monitored during the fluidization of four different types of liposomes, two of which represent  
248 optimal growth conditions and the other two stress conditions. In the presence of liposomes  
249 mimicking *O. oeni* membranes adapted to stress (stationary phase and ethanol adapted, the  
250 lipochaperone activity of Lo18 was established at higher temperature or abolished. Furthermore,  
251 these stress-adapted liposomes had the lowest phosphatidylglycerol content, suggesting that  
252 the electrostatic attraction of proteins by the membrane may be a more significant factor than  
253 membrane fluidity in lipochaperone activity. Conversely, for Lo18 membrane insertion,  
254 membrane fluidity appeared to be an important factor.

255 Indeed, although Lo18 is unable to insert into liposomes extracted from a culture of *L. plantarum*,  
256 having a lipid profile (for the main polar heads) similar to that of *O. oeni* culture in exponential  
257 phase, it retains lipochaperone activity. It is therefore plausible that Lo18, like human sHSPs  
258 HSPB1 and HSPB5 [12] or HSP16 from *S. pombe* [17], may be attracted first by polar head groups  
259 before interacting with specific membrane microdomains [45] via an as yet unknown mechanism,  
260 allowing it to reinforce its lipochaperone activity.

261 The results obtained in this study lead us to propose a model. During membrane fluidization,  
262 dimers from cytoplasmic oligomeric structures (which regularly undergo  
263 association/dissociation cycles) are attracted to the membrane. Hydrophobic and electrostatic  
264 forces could attract them towards lipids, in particular unsaturated and negatively charged  
265 phospholipids (notably oleic acid and phosphatidylglycerol) for which Lo18 has greater affinity.  
266 In particular, it appears that the contribution of electrostatic forces induced by the polar heads

267 of membrane phospholipids may influence the lipochaperone activity of Lo18, whereas forces of  
268 a hydrophobic type would influence the insertion of Lo18 into membranes, which is consistent  
269 with current understanding of membrane protein insertion [40].(Fig. 5).

270  
271 In conclusion, the present work contributes to a better understanding of the mechanisms of  
272 sHSPs and bacterial membrane interaction. Such understanding could allow the use the  
273 lipochaperone role of sHsps in different fields, such as in the agri-food industry, for example the  
274 resistance of *L. plantarum* to freeze drying processes [46] or in the medical field for the treatment  
275 of neurodegenerative diseases such as exudative retinopathy [47]

276  
277

## 278 **Material and methods**

### 279 Media and growth conditions

280 *O. oeni* ATCC BAA-1163 was grown in modified FT80 medium [48] at pH 5.3 and 28 °C in the  
281 presence or absence of 8% ethanol. *L. plantarum* WFS1 was grown in MRS medium (Condalab,  
282 Spain) at pH 6.2 and 28 °C.

### 283 Preparation of liposomes

284 *O. oeni* and *L. plantarum* cultures were grown to the exponential and/or stationary growth phase  
285 before lipids were extracted and purified according to Bligh and Dyer [49]. Liposomes were  
286 produced by adapting the method described by Maitre et al. 2012. [11]. The chloroform present  
287 in the lipid fraction was evaporated using a nitrogen flow. The lipids were then gently resuspended  
288 in 10 mL of 50 mM phosphate buffer, pH 7.0, previously heated to 55°C. After being sonicated  
289 twice for 2 min (Branson Ultrasonics™ CPX-952-138R, Branson Ultrasonics, Brookfield, CT, US),  
290 the lipid solution was rehydrated for 4 h at 55°C. The lipid particles were then extruded through a  
291 polycarbonate membrane with 1 µm-diameter pores to obtain the liposomes similar in size to *O.*  
292 *oeni* cells. The liposomes were stored at 4 °C for up to 1 week.

### 293 Fluidity Measurements

294 Fluorescence anisotropy measurements (reflecting the fluidity state of the membrane) were  
295 performed using a FLUOROLOG-3 spectrofluorometer (Jobin Yvon Inc, USA). Each measurement  
296 was performed at excitation and emission wavelengths of 360 nm and 431 nm, respectively. Two  
297 hundred and fifty µL of liposomes and 3 µM of 1,6-diphenyl-1,3,5 hexatriene (DPH) probe (Sigma  
298 Aldrich, St. Louis, US) were mixed in a quartz cuvette (10 mm optical path) to a final volume of 3  
299 mL. Measurements were performed on the liposome suspension in the presence or absence of  
300 Lo18 with a mass ratio of 1:2 (m/m) (Lo18/liposomes) following a temperature increase from 15  
301 to 84 °C (2 °C *per min* increase) controlled by a Peltier system (QNW TC1 temperature controller,  
302 Quantum Northwest, Liberty Lake, WA, USA). For each experiment, an anisotropy value was  
303 obtained every 14.6 s and calculated according to Shinitzky and Barenholz 1978[50]. Each  
304 experiment was performed in triplicate.

### 305 Synchrotron radiation circular dichroism (SRCD) spectroscopy

306 Circular dichroism spectra were collected on the DISCO beamline (Synchrotron SOLEIL, France)  
307 according to [51]. The instrument was calibrated using 99% pure (+) camphor-10-sulphonic acid  
308 (Sigma Aldrich, Saint-Louis, US) at 25 °C after each beam fill [52]. Lo18 at 140 µM was prepared  
309 in 50 mM sodium phosphate buffer, pH 7.0, alone or in the presence of liposomes at 250 µM.  
310 Then, 50 µL of sample was loaded into a 0.02 cm pathlength demountable cylindrical Suprasil  
311 quartz cell (Hellma, Germany) and subjected to a thermal scan from 15 °C to 84 °C with a step of



312 3 °C. Each dataset was collected from 262 nm to 176 nm, with an integration time of 1.2 s and a  
313 spectral bandwidth of 1 nm. Three scans of each sample and the equivalent baseline were  
314 collected. The sample spectrum was averaged across the three repeats, and the averaged  
315 baselines (buffer without protein) subtracted. Baseline-subtracted spectra were zeroed between  
316 250 and 260 nm. All the spectra were normalized according to the protein concentration and  
317 pathlength using the CDToolX software and deconvoluted using BeStSel online software [53].

318

319

#### Lipid Protein overlay assay

320 The interactions between lipids and Lo18 or modified proteins were observed by immunostaining,  
321 according to [54]. A drop of 2 µL of dipalmitoyl phosphatidylethanolamine (DPPE), dioleoyl  
322 phosphatidylethanolamine (DOPE), dioleoyl phosphatidic acid (DOPA), dipalmitoyl  
323 phosphatidylcholine (DPPC), dioleoyl phosphatidylcholine (DOPC), dipalmitoyl  
324 phosphatidylglycerol (DPPG), and dioleoylphosphatidylglycerol (DOPG) (Avanti polar, France) at  
325 1.5 mM was deposited on a PVDF membrane (Fisher scientific, USA). The membrane was blocked  
326 in TBS/Regilait 5%, 1 h at 70 rpm and washed three times for 5 min with TBS. It was then incubated  
327 with Lo18 or modified purified protein at 7.5 µg/mL and washed again three times. Afterward, the  
328 protein bound to the lipids was detected with antibodies against Lo18 (1/750), produced by  
329 Eurogenetec with mice, and against the primary antibody (1/2000) against mice antibodies by  
330 incubating the membrane for 1 h at 70 rpm for each antibody. Chemiluminescence was detected  
331 using the ECL reagent kit (Thermo Fisher, USA). A normalization step was added to quantify the  
332 interaction between Lo18 and the phospholipids. To do this, the proportion of phospholipids fixed  
333 to the PVDF membrane was measured by fluorescence imaging after 15 min incubation with 50  
334 mM of Nile Red staining. Then the signal intensity obtained for the immunolabeling measurement  
335 was adjusted to the signal obtained for the Nile Red staining.

336

#### Lipidomic analysis

337

##### Total fatty acids analysis by GCMS-NCI

338 Bligh and Dyer lipid extracts (50 µL) were mixed with 25 µL of a fatty acid internal standard mix  
339 (Avanti Polar Lipids, France) containing: 1146 ng of myristic acid-d3, 4973 ng of palmitic acid-d3,  
340 3703 ng of stearic acid-d3, 3174 ng of linoleic acid d4, 45.8 ng of arachidic acid-d3, 1632 ng of  
341 arachidonic acid-d8, 47.6 ng of behenic acid-d3, 476.1 ng of DHA-d5, 22.9 ng of Lignoceric-d4,  
342 and 17.6 ng of cerotic acid-d4. Total fatty acids were quantitated after alkaline hydrolysis by  
343 GCMS-NCI, as previously described [55]

344

##### Lipid analysis by LCMS2

345 Bligh and Dyer lipid extracts (200 µL) were dried under vacuum and mixed with an internal  
346 standard mix (50 µL) (CDN Isotopes, France and Cayman, France), (14:0)4CL (800 ng), (12:0)2DG  
347 (8 µg), and (21:0)2PC (50 ng). Sample (1 µL) was analyzed by LCMSMS using a Zorbax®Eclipse Plus  
348 C18 1.8 µm, 2.1 x 100 mm column maintained at 55 °C (Agilent Technologies).

349 Briefly, digalactosyldiacylglycerols (DGDG), monogalactosyldiacylglycerols (MGDG), and  
350 diacylglycerols (DG) were separated on a 1260 Infinity LC system (Agilent Technologies) with a  
351 gradient of mobile phase A (acetonitrile/water/1M ammonium formate (60/39/1 v/v/v) with 0.1%  
352 formic acid), and mobile phase B (isopropanol/acetonitrile/1M ammonium formate (90/9/1 v/v/v)  
353 with 0.1% formic acid) [56] at a flow rate of 0.4 mL/min set as follows: 1 min hold at 50% B; 50-  
354 60% B in 4 min; 60-85% B in 10 min; 85-99% B in 1 min; 2 min hold at 99%, 99%-50% ramp-down  
355 in 0.1 min and maintained at 50% B for 3.9 min. Acquisition was carried out on a 6460 Triple

356 Quadrupole (Agilent Technologies) equipped with an ESI Jet stream source (temperature 250 °C,  
357 nebulizer 20 L/min, sheath gas 11 L/min, sheath gas temperature 220 °C, capillary 3500 V, nozzle  
358 1000 V) operating in positive Single Reaction Monitoring (SRM) mode (fragmentor 148 V, collision  
359 energy 23 V). Transitions were set as the neutral loss of 359 Da for DGDG or 197 Da for MGDG  
360 from their respective [M+NH<sub>4</sub>]<sup>+</sup> ions [57] DG (as NH<sub>4</sub><sup>+</sup> adducts) were quantified according to the  
361 sum of the signal resulting from the neutral loss of either their sn-1 or sn-2 fatty acid. Finally, lipid  
362 concentrations were determined by calculating their relative response to (12:0)2DG used as  
363 internal standard.

364 Phosphatidylglycerols (PG) and lysyl-phosphatidylglycerols (lysyl-PG) were separated with the  
365 same mobile phases and column as for DGs, and the elution gradient used was set as follows: 2  
366 min hold at 50% B; 50-99% B in 14 min; 2 min hold at 99%, 99%-50% ramp-down in 0.1 min; return  
367 to initial conditions in 1.9 min. Acquisition was carried out on a 6460 Triple Quadrupole (Agilent  
368 Technologies) equipped with an ESI Jet stream source (temperature 200 °C, nebulizer 20 L/min,  
369 sheath gas 11 L/min, sheath gas temperature 220 °C, capillary 3500 V, nozzle 1000 V) operating  
370 in positive Single Reaction Monitoring (SRM) mode (fragmentor/collector 116 V/13 V and 300 V/34  
371 V for PG and Lysyl-PG respectively). Transitions were set as the neutral loss of 189 Da or 300 Da  
372 for [PG+NH<sub>4</sub>]<sup>+</sup> and [Lysyl-PG+H]<sup>+</sup> ions respectively. Lipid concentrations were determined by  
373 calculating relative response ratios with regards to (12:0)2DG used as internal standard.

374 The analysis of cardiolipins (CL) and phosphatidylcholines (PC) was performed as previously  
375 described [58, 59] except that a Vanquish LC system, coupled to a triple-stage quadrupole (TSQ)  
376 Altis mass spectrometer equipped with a heated electrospray ionization source (Thermo  
377 Scientific) was used (sheath gas, 50 arb; auxiliary gas, 10 arb; sweep gas, 1 arb; ion transfer tube  
378 temperature, 325 °C; vaporizer temperature, 350 °C and ion spray voltage, 3500 V (+), and  
379 2500 V (-)). Lipid concentrations for all the quantified lipid classes were expressed in pmol/mg of  
380 Bligh and Dyer extract.

#### 381 Statistical analysis

382 For each condition tested on fluorescence anisotropy, immunolabelling, lipidic profile, and  
383 secondary structure analysis were performed using three independent measurements. The  
384 anisotropy values obtained were normalized to be expressed in percentage compared to the  
385 initial value at 15 °C. Statistical analyses were performed by the statistical RStudio software  
386 (version 1.2.5033). The normality of the distribution and homogeneity of the variances of each  
387 condition were tested by the Shapiro-Wilk test and the Bartlett test, respectively. Then, a non-  
388 parametric Kruskal-Wallis test was used to compare the samples with a significance level of  $\alpha =$   
389 0.05. All the statistical tests were considered significant at a p-value <0.05.

390

#### 391 Acknowledgments

392 The present work was supported by the Regional Council of Bourgogne- Franche-Comté  
393 Bourgogne grant number 2021Y-09559, and the Ministère de l'Enseignement supérieur, de la  
394 Recherche et de l'Innovation, grant number MESR 2020-04. The authors would like to thank the  
395 Dimacell Platform (Agrosup Dijon, INRA, INSERM, Univ. Bourgogne Franche-Comté, F-21000  
396 Dijon France), the lipidomic platform (LAP, Université de Bourgogne, Dijon, France), and the  
397 Synchrotron SOLEIL (Saint-Aubin, France) for X-ray beamtime on the DISCO beamline (project  
398 #20220067). We would also like to thank Accent Europe for proofreading the English text.  
399

400 **Conflicts of Interest:** The authors declare no conflict of interest.

401 **Author contribution:** T. B. and S. W: Conceptualization, T. B., and S. W: Methodology, T. B.  
402 Formal analysis, T. B. and S. W.: Investigation, T. B., S. W and F. W.: Resources, T. B. and S. W :  
403 Writing – Original Draft, T. B, S. W., F. W., , P. F.-V. and S. C. : Writing – Review & Editing; S. W.:  
404 Validation, Project administration and Funding acquisition

405 **Data availability:** The datasets generated during and/or analysed during the current study are  
406 available from the corresponding author on reasonable request.

407  
408

#### 409 **References:**

- 410 1 Chu-Ky, S., Tourdot-Marechal, R., Marechal, P.-A. and Guzzo, J. (2005) Combined cold, acid,  
411 ethanol shocks in *Oenococcus oeni*: Effects on membrane fluidity and cell viability.  
412 *Biochimica et Biophysica Acta (BBA) - Biomembranes* **1717**, 118–124  
413 <https://doi.org/10.1016/j.bbamem.2005.09.015>
- 414 2 Da Silveira, M. G., Golovina, E. A., Hoekstra, F. A., Rombouts, F. M. and Abee, T. (2003)  
415 Membrane fluidity adjustments in ethanol-stressed *Oenococcus oeni* cells. *AEM* **69**, 5826–  
416 5832 <https://doi.org/10.1128/AEM.69.10.5826-5832.2003>
- 417 3 Wen-ying, Z. and Zhen-kui, K. (2013) Advanced progress on adaptive stress response of  
418 *Oenococcus oeni*. *Journal of Northeast Agricultural University (English Edition)* **20**, 91–96  
419 [https://doi.org/10.1016/S1006-8104\(13\)60015-X](https://doi.org/10.1016/S1006-8104(13)60015-X)
- 420 4 D’Amico, S., Collins, T., Marx, J., Feller, G., Gerday, C. and Gerday, C. (2006) Psychrophilic  
421 microorganisms: challenges for life. *EMBO Rep* **7**, 385–389  
422 <https://doi.org/10.1038/sj.embor.7400662>
- 423 5 Olguín, N., Bordons, A. and Reguant, C. (2009) Influence of ethanol and pH on the gene  
424 expression of the citrate pathway in *Oenococcus oeni*. *Food Microbiology* **26**, 197–203  
425 <https://doi.org/10.1016/j.fm.2008.09.004>
- 426 6 Cisolotto, B., Scariot, F. J., Vivian Schwarz, L., Mattos Rocha, R. K., Longaray Delamare, A. P.  
427 and Echeverrigaray, S. (2021) Yeast stress and death caused by the synergistic effect of  
428 ethanol and SO<sup>2</sup> during the second fermentation of sparkling wines. *OENO One* **55**, 49–69  
429 <https://doi.org/10.20870/oeno-one.2021.55.4.4809>
- 430 7 Gonzalez, R. and Morales, P. (2022) Truth in wine yeast. *Microbial Biotechnology* **15**, 1339–  
431 1356 <https://doi.org/10.1111/1751-7915.13848>
- 432 8 Mogk, A., Ruger-Herreros, C. and Bukau, B. (2019) Cellular functions and mechanisms of  
433 action of small heat shock proteins. *Annu. Rev. Microbiol.* **73**, 89–110  
434 <https://doi.org/10.1146/annurev-micro-020518-115515>
- 435 9 Haslbeck, M. and Vierling, E. (2015) A first line of stress defense: small heat shock proteins  
436 and their function in protein homeostasis. *Journal of Molecular Biology* **427**, 1537–1548  
437 <https://doi.org/10.1016/j.jmb.2015.02.002>
- 438 10 Obuchowski, I. and Liberek, K. (2020) Small but mighty: a functional look at bacterial sHSPs.  
439 *Cell Stress and Chaperones* **25**, 593–600 <https://doi.org/10.1007/s12192-020-01094-0>
- 440 11 Maitre, M., Weidmann, S., Rieu, A., Fenel, D., Schoehn, G., Ebel, C., et al. (2012) The  
441 oligomer plasticity of the small heat-shock protein Lo18 from *Oenococcus oeni* influences  
442 its role in both membrane stabilization and protein protection. *Biochemical Journal* **444**, 97–  
443 104 <https://doi.org/10.1042/BJ20120066>
- 444 12 De Maio, A., Cauvi, D. M., Capone, R., Bello, I., Egberts, W. V., Arispe, N., et al. (2019) The  
445 small heat shock proteins, HSPB1 and HSPB5, interact differently with lipid membranes.  
446 *Cell Stress and Chaperones* **24**, 947–956 <https://doi.org/10.1007/s12192-019-01021-y>
- 447 13 Nitta, K., Suzuki, N., Honma, D., Kaneko, Y. and Nakamoto, H. (2005) Ultrastructural  
448 stability under high temperature or intensive light stress conferred by a small heat shock  
449 protein in cyanobacteria. *FEBS Letters* **579**, 1235–1242  
450 <https://doi.org/10.1016/j.febslet.2004.12.095>

- 451 14 Török, Z., Goloubinoff, P., Horváth, I., Tsvetkova, N. M., Glatz, A., Balogh, G., et al. (2001)  
452 *Synechocystis* HSP17 is an amphitropic protein that stabilizes heat-stressed membranes  
453 and binds denatured proteins for subsequent chaperone-mediated refolding. *Proceedings*  
454 *of the National Academy of Sciences* **98**, 3098–3103  
455 <https://doi.org/10.1073/pnas.051619498>
- 456 15 De Maio, A. and Hightower, L. E. (2021) Heat shock proteins and the biogenesis of cellular  
457 membranes. *Cell Stress and Chaperones* **26**, 15–18 [https://doi.org/10.1007/s12192-020-](https://doi.org/10.1007/s12192-020-01173-2)  
458 [01173-2](https://doi.org/10.1007/s12192-020-01173-2)
- 459 16 Kim, D. H., Xu, Z.-Y., Na, Y. J., Yoo, Y.-J., Lee, J., Sohn, E.-J., et al. (2011) Small heat shock  
460 protein Hsp17.8 functions as an Akr2a cofactor in the targeting of chloroplast outer  
461 membrane proteins in arabidopsis. *Plant Physiology* **157**, 132–146  
462 <https://doi.org/10.1104/pp.111.178681>
- 463 17 Glatz, A., Pilbat, A.-M., Németh, G. L., Vince-Kontár, K., Jós vay, K., Hunya, Á., et al. (2016)  
464 Involvement of small heat shock proteins, trehalose, and lipids in the thermal stress  
465 management in *Schizosaccharomyces pombe*. *Cell Stress and Chaperones* **21**, 327–338  
466 <https://doi.org/10.1007/s12192-015-0662-4>
- 467 18 Rocchetti, M. T., Bellanger, T., Trecca, M. I., Weidmann, S., Scrima, R., Spano, G., et al.  
468 (2023) Molecular chaperone function of three small heat-shock proteins from a model  
469 probiotic species. *Cell Stress and Chaperones* **28**, 79–89 [https://doi.org/10.1007/s12192-](https://doi.org/10.1007/s12192-022-01309-6)  
470 [022-01309-6](https://doi.org/10.1007/s12192-022-01309-6)
- 471 19 Delmas, F., Pierre, F., Divies, C. and Guzzo, J. (2001) Biochemical and physiological studies  
472 of the small heat shock protein Lo18 from the lactic acid bacterium *Oenococcus oeni*.  
473 *Journal of molecular microbiology and biotechnology* **3**, 601–610
- 474 20 Coucheney, F., Gal, L., Beney, L., Lherminier, J., Gervais, P. and Guzzo, J. (2005) A small  
475 HSP, Lo18, interacts with the cell membrane and modulates lipid physical state under heat  
476 shock conditions in a lactic acid bacterium. *Biochimica et Biophysica Acta (BBA) -*  
477 *Biomembranes* **1720**, 92–98 <https://doi.org/10.1016/j.bbamem.2005.11.017>
- 478 21 Jobin, M.-P., Delmas, F., Garmyn, D., Diviès, C. and Guzzo, J. (1997) Molecular  
479 characterization of the gene encoding an 18-kilodalton small heat shock protein associated  
480 with the membrane of *Leuconostoc oenos*. *Applied and environmental microbiology* **63**,  
481 609–614 <https://doi.org/10.1128/AEM.63.2.609-614.1997>
- 482 22 Guzzo, J., Delmas, F., Pierre, F., Jobin, M.-P., Samyn, B., Van Beeumen, J., et al. (1997) A  
483 small heat shock protein from *Leuconostoc oenos* induced by multiple stresses and during  
484 stationary growth phase. *Letters in Applied Microbiology* **24**, 393–396  
485 <https://doi.org/10.1046/j.1472-765X.1997.00042.x>
- 486 23 Maitre, M., Weidmann, S., Dubois-Brissonnet, F., David, V., Covès, J. and Guzzo, J. (2014)  
487 Adaptation of the wine bacterium *Oenococcus oeni* to ethanol stress: role of the small heat  
488 shock protein Lo18 in membrane integrity. *Appl. Environ. Microbiol.* (Pettinari, M. J., ed.) **80**,  
489 2973–2980 <https://doi.org/10.1128/AEM.04178-13>
- 490 24 Weidmann, S., Rieu, A., Rega, M., Coucheney, F. and Guzzo, J. (2010) Distinct amino acids  
491 of the *Oenococcus oeni* small heat shock protein Lo18 are essential for damaged protein  
492 protection and membrane stabilization: Protein protection and membrane stabilization by  
493 smHsp Lo18. *FEMS Microbiology Letters* no-no [https://doi.org/10.1111/j.1574-](https://doi.org/10.1111/j.1574-6968.2010.01999.x)  
494 [6968.2010.01999.x](https://doi.org/10.1111/j.1574-6968.2010.01999.x)
- 495 25 Bellanger, T. and Weidmann, S. (2023) Is the lipochaperone activity of sHSP a key to the  
496 stress response encoded in its primary sequence? *Cell Stress and Chaperones* **28**, 21–33  
497 <https://doi.org/10.1007/s12192-022-01308-7>
- 498 26 Bellanger, T., da Silva Barreira, D., Wien, F., Delarue, P., Senet, P., Rieu, A., et al. (2023)  
499 Significant influence of four highly conserved amino-acids in lipochaperon-active sHsps on  
500 the structure and functions of the Lo18 protein. *Sci Rep* **13**, 19036  
501 <https://doi.org/10.1038/s41598-023-46306-6>

- 502 27 O’Leary, W. M. (1962) THE FATTY ACIDS OF BACTERIA. *Bacteriol Rev* **26**, 421–447  
503 <https://doi.org/10.1128/br.26.4.421-447.1962>
- 504 28 Csoboz, B., Gombos, I., Kóta, Z., Dukic, B., Klement, É., Varga-Zsíros, V., et al. (2022) The  
505 small heat shock protein, HSPB1, interacts with and modulates the physical structure of  
506 membranes. *IJMS* **23**, 7317 <https://doi.org/10.3390/ijms23137317>
- 507 29 Denich, T. J., Beaudette, L. A., Lee, H. and Trevors, J. T. (2003) Effect of selected  
508 environmental and physico-chemical factors on bacterial cytoplasmic membranes. *Journal*  
509 *of Microbiological Methods* **52**, 149–182 [https://doi.org/10.1016/S0167-7012\(02\)00155-0](https://doi.org/10.1016/S0167-7012(02)00155-0)
- 510 30 Beney, L. and Gervais, P. (2001) Influence of the fluidity of the membrane on the response of  
511 microorganisms to environmental stresses. *Applied Microbiology and Biotechnology* **57**, 34–  
512 42 <https://doi.org/10.1007/s002530100754>
- 513 31 Bouix, M. and Ghorbal, S. (2015) Rapid assessment of *Oenococcus oeni* activity by  
514 measuring intracellular pH and membrane potential by flow cytometry, and its application  
515 to the more effective control of malolactic fermentation. *International Journal of Food*  
516 *Microbiology* **193**, 139–146 <https://doi.org/10.1016/j.ijfoodmicro.2014.10.019>
- 517 32 Fonseca, F., Pénicaud, C., Tymczynsyn, E. E., Gómez-Zavaglia, A. and Passot, S. (2019)  
518 Factors influencing the membrane fluidity and the impact on production of lactic acid  
519 bacteria starters. *Appl Microbiol Biotechnol* **103**, 6867–6883  
520 <https://doi.org/10.1007/s00253-019-10002-1>
- 521 33 Zhukovsky, M. A., Filograna, A., Luini, A., Corda, D. and Valente, C. (2019) Phosphatidic acid  
522 in membrane rearrangements. *FEBS Letters* **593**, 2428–2451 <https://doi.org/10.1002/1873-3468.13563>
- 523
- 524 34 Grogan, D. W. and Cronan, J. E. (1997) Cyclopropane ring formation in membrane lipids of  
525 bacteria. *Microbiology and Molecular Biology Reviews*, American Society for Microbiology  
526 **61**, 429–441 <https://doi.org/10.1128/membr.61.4.429-441.1997>
- 527 35 Bouix, M. and Ghorbal, S. (2017) Assessment of bacterial membrane fluidity by flow  
528 cytometry. *Journal of Microbiological Methods* **143**, 50–57  
529 <https://doi.org/10.1016/j.mimet.2017.10.005>
- 530 36 Cronan, J. E. (2002) Phospholipid modifications in bacteria. *Current Opinion in Microbiology*  
531 **5**, 202–205 [https://doi.org/10.1016/S1369-5274\(02\)00297-7](https://doi.org/10.1016/S1369-5274(02)00297-7)
- 532 37 Tsvetkova, N. M., Horvath, I., Torok, Z., Wolkers, W. F., Balogi, Z., Shigapova, N., et al. (2002)  
533 Small heat-shock proteins regulate membrane lipid polymorphism. *Proceedings of the*  
534 *National Academy of Sciences* **99**, 13504–13509 <https://doi.org/10.1073/pnas.192468399>
- 535 38 Mitra, A., Bhakta, K., Kar, A., Roy, A., Mohid, S. A., Ghosh, A., et al. (2023) Insight into the  
536 biochemical and cell biological function of an intrinsically unstructured heat shock protein,  
537 Hsp12 of *Ustilago maydis*. *Molecular Plant Pathology* **24**, 1063–1077  
538 <https://doi.org/10.1111/mpp.13350>
- 539 39 Bürck, J., Wadhwani, P., Fanghänel, S. and Ulrich, A. S. (2016) Oriented circular dichroism: a  
540 method to characterize membrane-active peptides in oriented lipid bilayers. *Acc. Chem.*  
541 *Res.* **49**, 184–192 <https://doi.org/10.1021/acs.accounts.5b00346>
- 542 40 Davletov, B., Perisic, O. and Williams, R. L. (1998) Calcium-dependent Membrane  
543 Penetration Is a Hallmark of the C2 Domain of Cytosolic Phospholipase A2 Whereas the  
544 C2A Domain of Synaptotagmin Binds Membranes Electrostatically. *Journal of Biological*  
545 *Chemistry* **273**, 19093–19096 <https://doi.org/10.1074/jbc.273.30.19093>
- 546 41 Balogi, Z., Cheregi, O., Giese, K. C., Juhász, K., Vierling, E., Vass, I., et al. (2008) A mutant  
547 small heat shock protein with increased thylakoid association provides an elevated  
548 resistance against UV-B Damage in *Synechocystis* 6803. *Journal of Biological Chemistry*  
549 **283**, 22983–22991 <https://doi.org/10.1074/jbc.M710400200>
- 550 42 Horváth, I., Multhoff, G., Sonnleitner, A. and Vigh, L. (2008) Membrane-associated stress  
551 proteins: More than simply chaperones. *Biochimica et Biophysica Acta (BBA) -*  
552 *Biomembranes* **1778**, 1653–1664 <https://doi.org/10.1016/j.bbamem.2008.02.012>

- 553 43 Lenaz, G. (1987) Lipid fluidity and membrane protein dynamics. *Bioscience Reports* **7**, 823–  
554 837 <https://doi.org/10.1007/BF01119473>
- 555 44 Balogi, Z., Török, Z., Balogh, G., Jósvay, K., Shigapova, N., Vierling, E., et al. (2005) “Heat  
556 shock lipid” in cyanobacteria during heat/light-acclimation. *Archives of Biochemistry and*  
557 *Biophysics* **436**, 346–354 <https://doi.org/10.1016/j.abb.2005.02.018>
- 558 45 Nickels, J. D., Hogg, J., Corder, D. and Katsaras, J. (2020) Lipid rafts in bacteria: structure  
559 and function. in health consequences of microbial interactions with hydrocarbons, oils, and  
560 lipids (Goldfine, H., ed.), pp 3–32, Springer International Publishing, Cham  
561 [https://doi.org/10.1007/978-3-030-15147-8\\_3](https://doi.org/10.1007/978-3-030-15147-8_3)
- 562 46 Arena, M. P., Capozzi, V., Longo, A., Russo, P., Weidmann, S., Rieu, A., et al. (2019) The  
563 phenotypic analysis of *Lactobacillus plantarum* sHSP mutants reveals a potential role for  
564 hsp1 in cryotolerance. *Front. Microbiol.* **10**, 838 <https://doi.org/10.3389/fmicb.2019.00838>
- 565 47 Tóth, M. E., Sántha, M., Penke, B. and Vígh, L. (2015) How to stabilize both the proteins and  
566 the membranes: diverse effects of shsp in neuroprotection. in the big book on Small Heat  
567 Shock Proteins (Tanguay, R. M., and Hightower, L. E., eds.), pp 527–562, Springer  
568 International Publishing, Cham [https://doi.org/10.1007/978-3-319-16077-1\\_23](https://doi.org/10.1007/978-3-319-16077-1_23)
- 569 48 Cavin, J. F., Prevost, H., Lin, J., Schmitt, P. and Divies, C. (1989) Medium for Screening  
570 *Leuconostoc oenos* Strains Defective in Malolactic Fermentation. *Appl Environ Microbiol*  
571 **55**, 751–753
- 572 49 Bligh, E. G. and Dyer, W. J. (1959) A rapid method of total lipid extraction and purification -  
573 PubMed. *Canadian journal of biochemistry and physiology* **37**, 911–917
- 574 50 Shinitzky, M. and Barenholz, Y. (1978) Fluidity parameters of lipid regions determined by  
575 fluorescence polarization. *Biochimica et Biophysica Acta (BBA) - Reviews on*  
576 *Biomembranes* **515**, 367–394 [https://doi.org/10.1016/0304-4157\(78\)90010-2](https://doi.org/10.1016/0304-4157(78)90010-2)
- 577 51 Evans, P., Wyatt, K., Wistow, G. J., Bateman, O. A., Wallace, B. A. and Slingsby, C. (2004)  
578 The P23T cataract mutation causes loss of solubility of folded  $\gamma$ D-Crystallin. *Journal of*  
579 *Molecular Biology* **343**, 435–444 <https://doi.org/10.1016/j.jmb.2004.08.050>
- 580 52 Miles, A. J., Wien, F. and Wallace, B. A. (2004) Redetermination of the extinction coefficient  
581 of camphor-10-sulfonic acid, a calibration standard for circular dichroism spectroscopy.  
582 *Anal Biochem* **335**, 338–339 <https://doi.org/10.1016/j.ab.2004.08.035>
- 583 53 Micsonai, A., Moussong, É., Wien, F., Boros, E., Vadász, H., Murvai, N., et al. (2022)  
584 BeStSel: webserver for secondary structure and fold prediction for protein CD  
585 spectroscopy. *Nucleic Acids Res* **50**, W90–W98 <https://doi.org/10.1093/nar/gkac345>
- 586 54 Dowler, S., Kular, G. and Alessi, D. R. (2002) Protein Lipid Overlay Assay. *Science Signaling*  
587 **11** <https://doi.org/10.1126/stke.2002.129.pl6>
- 588 55 Blondelle, J., Pais De Barros, J.-P., Pilot-Storck, F. and Tiret, L. (2017) Targeted lipidomic  
589 analysis of myoblasts by GC-MS and LC-MS/MS. In *Skeletal Muscle Development* (Ryall, J.  
590 G., ed.), pp 39–60, Springer New York, New York, NY [https://doi.org/10.1007/978-1-4939-7283-8\\_4](https://doi.org/10.1007/978-1-4939-7283-8_4)
- 592 56 Cajka, T., Hricko, J., Rudl Kulhava, L., Paucova, M., Novakova, M. and Kuda, O. (2023)  
593 Optimization of mobile phase modifiers for fast lc-ms-based untargeted metabolomics and  
594 lipidomics. *IJMS* **24**, 1987 <https://doi.org/10.3390/ijms24031987>
- 595 57 Carriot, N., Paix, B., Greff, S., Viguier, B., Briand, J.-F. and Culioli, G. (2021) Integration of  
596 LC/MS-based molecular networking and classical phytochemical approach allows in-depth  
597 annotation of the metabolome of non-model organisms - The case study of the brown  
598 seaweed *Taonia atomaria*. *Talanta* **225**, 121925  
599 <https://doi.org/10.1016/j.talanta.2020.121925>
- 600 58 Vial, G., Chauvin, M.-A., Bendridi, N., Durand, A., Meugnier, E., Madec, A.-M., et al. (2015)  
601 Imeglimin Normalizes glucose tolerance and insulin sensitivity and improves mitochondrial  
602 function in liver of a high-fat, high-sucrose diet mice model. *Diabetes* **64**, 2254–2264  
603 <https://doi.org/10.2337/db14-1220>

604 59 Cotte, A. K., Cottet, V., Aires, V., Mouillot, T., Rizk, M., Vinault, S., et al. (2019) Phospholipid  
605 profiles and hepatocellular carcinoma risk and prognosis in cirrhotic patients. *Oncotarget*  
606 **10**, 2161–2172 <https://doi.org/10.18632/oncotarget.26738>

607  
608

609 **Legends:**

610 Fig. 1: Lipid affinity test of Lo18. Immunolabeling measurements were performed on Lo18 and  
611 several common phospholipids: unsaturated (dioleoyl, DO-) or saturated (dipalmitoyl, DP-) lipids  
612 with neutral (phosphatidylethanolamine, -PE and phosphatidylcholine, -PC) or negative  
613 (phosphatidic acid, -PA and phosphatidylglycerol, -PG) charged head groups. The intensity of the  
614 signal obtained after hybridization with Lo18 was normalized with the number of phospholipids  
615 fixed to the PVDF membrane. The data represent the means and SE of three independent  
616 experiments and were analyzed statistically by the Kruskal-Wallis nonparametric test.

617 Fig. 2: Lipidic composition of the liposomes used. Lipidic profiles of (i) *O. oeni* liposomes in  
618 exponential, stationary, or 36 h ethanol-adapted culture, or (ii) *L. plantarum* liposomes.  
619 Proportion of polar head group type (A) and fatty acids (B) of each liposome. The data represent  
620 the means and SE of three independent experiments and were analyzed statistically by Kruskal-  
621 Wallis nonparametric test.

622

623 Fig. 3: Lipo-chaperone activity of Lo18 according to the lipidic substrate. Measure of fluorescence  
624 anisotropy of DPH inserted into liposomes of: (i) *O. oeni* in the exponential phase (circle), the  
625 stationary phase (square), or 36 h ethanol-adapted culture (inverted triangle), or (ii) *L. plantarum*  
626 liposomes (triangle) during thermal ramping between 15 to 60°C in the absence (white symbols)  
627 or presence of Lo18 (colored symbols). The data represent the means and SE of three  
628 independent experiments and were analyzed statistically by the Mann-Whitney U-test.

629

630

631 Fig. 4: Secondary structure modification of Lo18 in interaction with liposomes of –i) *O. oeni* in  
632 exponential phase, stationary phase or 36h ethanol-adapted culture or (ii) *L. plantarum*  
633 liposomes. Proportion of secondary structure,  $\alpha$ -helix and  $\beta$ -sheet (A) SRCD spectra on 190-240  
634 nm wavelength at 15 °C (B) and 45°C (C) of Lo18 alone (black) or in the presence of liposomes  
635 from *O. oeni* culture in exponential phase (purple), stationary phase (blue) or 36h ethanol-  
636 adapted culture (turquoise) and *L. plantarum* culture (orange) (A). The data represent the means  
637 and SE of three independent experiments and were analyzed statistically by Kruskal-Wallis  
638 nonparametric test,  $pV < 0.05$ .

639

640 Fig. 5: Part of the mechanisms by which membrane lipids interact with Lo18. Summary table of  
641 influence of lipid environment and physiological state of membranes on lipo-chaperone activity,  
642 secondary structure, interaction and insertion of Lo18 with membrane (A). Schematic illustration  
643 of Lo18-membrane interaction (B). During an association/dissociation cycle of Lo18 oligomeric  
644 subunits, the protein may be attracted to the membrane by electrostatic and/or hydrophobic  
645 forces, allowing the protein to chaperone and/or insert into the membrane.

646

647 Supplementary data, table S1: Lipidomic analysis of the four liposomes used during the  
648 experiments. Data corresponding to means  $\pm$  SE and statistical analysis for each line.  
649 Measurements were replicated three times and analyzed by Kruskal-Wallis statistical test (P-  
650 value < 0.05).

651

652 Supplementary data, table S2: Anisotropy measurement of liposomes of (i) *O. oeni* in the  
653 exponential phase and stationary phase, or in ethanol-adapted culture or (ii) *L. plantarum* culture  
654 during thermal ramping between 15 to 65 °C in the absence or presence of Lo18. The data present  
655 the means of three independent experiments.

656

657 Supplementary data, Fig. S1: Lipid staining by 50 mM of Nile Red of several common  
658 phospholipids: unsaturated (dioleoyl, DO-) or saturated (dipalmitoyl, DP-) lipids with neutral  
659 (phosphatidylethanolamine, -PE and phosphatidylcholine, -PC) or negative (phosphatidic acid, -  
660 PA and phosphatidylglycerol, -PG) charged head group (A). Immunolabeling interaction between  
661 Lo18 and several common phospholipids (B). The membrane presented corresponds to an  
662 experiment representative of three independent measurements.

663



Figure 1

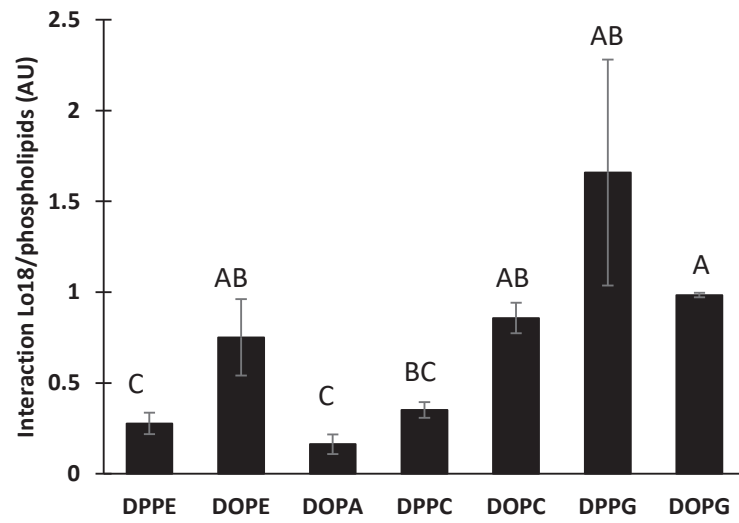


Figure 2

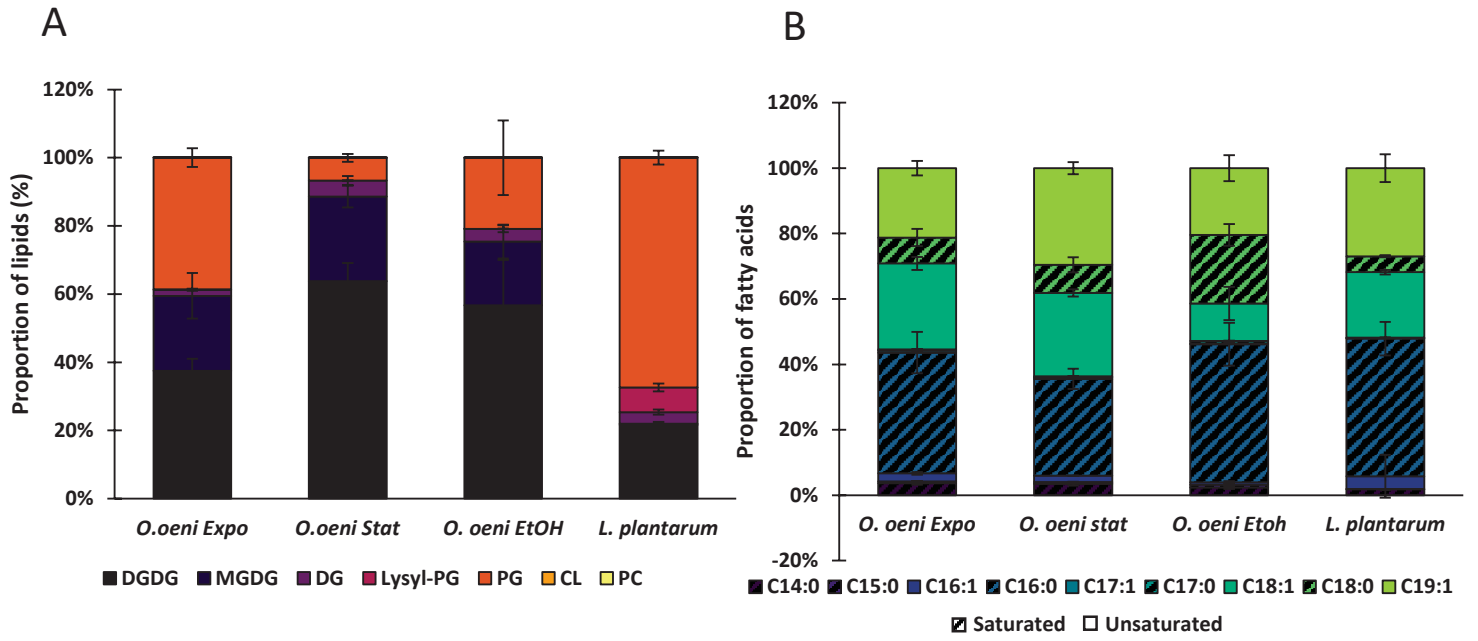


Figure 3

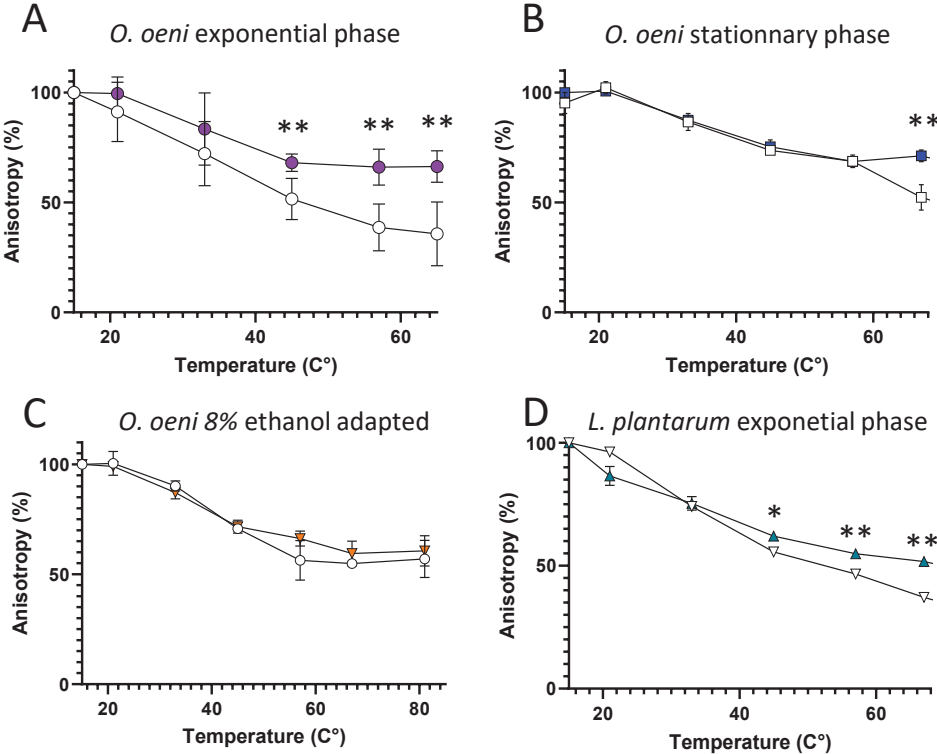


Figure 4

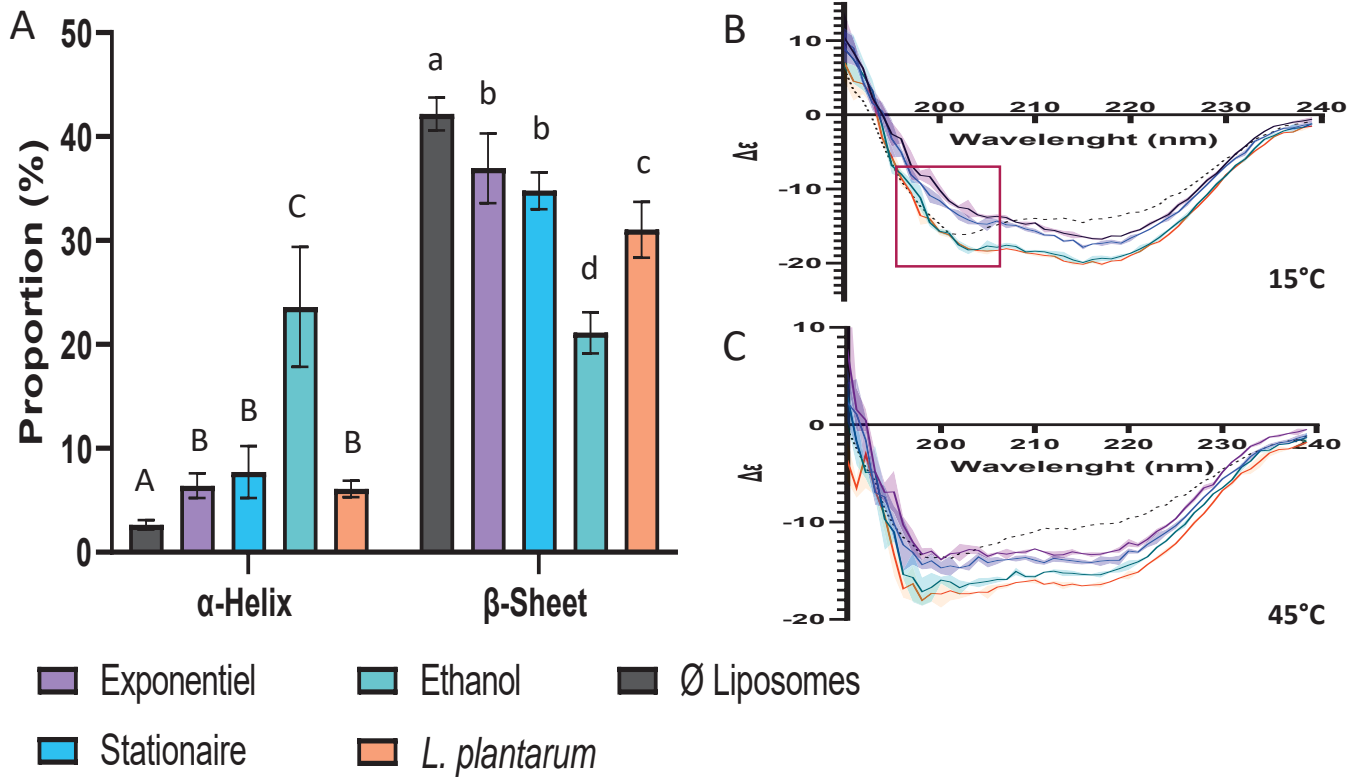
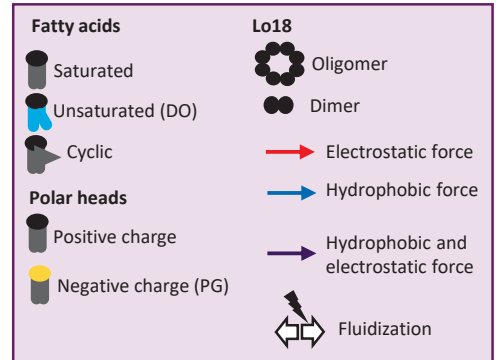


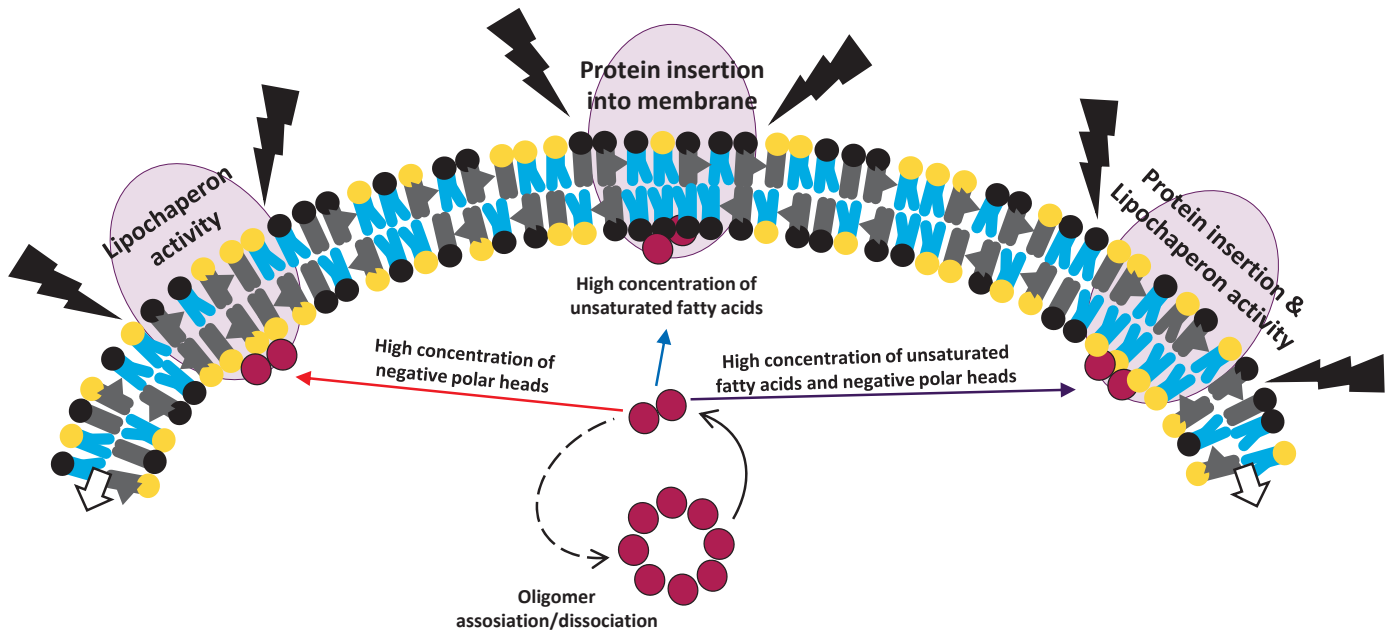
Figure 5

A

Microorganisms	<i>O. oeni</i>		<i>L. plantarum</i>	
Growth phase	Exponential	Stationary	Ethanol-adapted	Exponential
Lipids composition	PG+;DO+	PG-;DO+	PG-;DO-	PG+;DO-
Lipo-chaperon activity	++	+/-	-	++
Protein structures change ( $\alpha$ ; $\beta$ )	+/-	+/-	++/-	+/-
Insertion	+	+	-	-



B



# Supplementary data, Table S1

	<i>O. oeni</i> Exponential	<i>O. oeni</i> Stationary	<i>O. oeni</i> Ethanol 8%	<i>L. plantarum</i>	
Fatty acids (%)	<b>C14:0</b>	3.7 ± 0.5 A	3.5 ± 0.5 A	2.3 ± 0.4 AB	1.8 ± 0.2 B
	<b>C15:0</b>	0.6 ± 0.1 A	0.5 ± 0.1 A	0.8 ± 0.1 A	0.1 ± 0 B
	<b>C16:1</b>	2.4 ± 0.6 A	1.9 ± 0.5 A	0.8 ± 0.3 A	3.9 ± 0.8 B
	<b>C16:0</b>	36.9 ± 6.3 A	29.6 ± 3.1 A	42.2 ± 6.5 A	42.1 ± 5.1 A
	<b>C17:1</b>	0.6 ± 0.1 A	0.4 ± 0.1 AB	0.3 ± 0.1 BC	0.2 ± 0.1 C
	<b>C17:0</b>	0.4 ± 0.1 B	0.4 ± 0.1 B	0.7 ± 0.1 A	0.1 ± 0 C
	<b>C18:1</b>	26.3 ± 2 A	25.5 ± 1.1 A	11.5 ± 5.1 B	20 ± 0.7 B
	<b>C18:0</b>	7.9 ± 2.7 A	8.6 ± 2.3 A	21 ± 3.3 B	4.9 ± 0.3 A
	<b>C19:1</b>	21.2 ± 2.2 A	29.6 ± 1.9 A	20.4 ± 3.9 A	26.9 ± 4.2 A
Polar head groups (%)	<b>DGDG</b>	37.5 ± 33.5 AB	63.8 ± 5.3 A	56.7 ± 13.3 A	21.6 ± 0.9 B
	<b>MGDG</b>	22 ± 6.7 A	24.8 ± 3.2 A	18.7 ± 4.9 A	0.3 ± 0.1 B
	<b>DG</b>	1.7 ± 0.3 A	4.7 ± 1.3 A	3.7 ± 1.1 A	3.4 ± 0.7 A
	<b>Lysyl-PG</b>	0.2 ± 0.2 A	0 ± 0 A	0 ± 0 A	7.2 ± 1.1 B
	<b>PG</b>	38.6 ± 2.7 AB	6.7 ± 1.2 C	20.8 ± 10.9 BC	67.4 ± 2 A
	<b>CL</b>	0.009 ± 0.003 A	0.05 ± 0.01 B	0.02 ± 0.008 AB	0.002 ± 0.0005 C
	<b>PC</b>	0.0001 ± 0.00008 A	0.00006 ± 0.000004 A	0.0003 ± 0.0002 A	0.0007 ± 0.0001 B

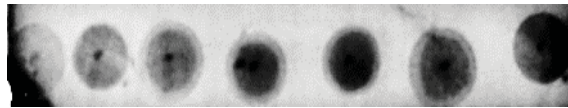
## Supplementary data, Table S2

		<i>O. oeni</i>			<i>L. plantarum</i>
Condition		Exponential	Stationary	Ethanol-adapted	Exponential
Anisotropy without Lo18	15°C	0.189	0.185	0.201	0.186
	65°C	0.070	0.105	0.108	0.070
	Rate of fluidification (%)	-63.0	-43.4	-46.2	-62.3
	Slope	-0.0024	-0.0016	-0.0019	-0.0023
Anisotropy with Lo18	15°C	0.220	0.228	0.239	0.208
	65°C	0.155	0.161	0.144	0.103
	Rate of fluidification (%)	-29.5	-29.2	-39.8	-50.5
	Slope	-0.0013	-0.0013	-0.0019	-0.0021

# Supplementary data, Figure S1

A

Nil Red coloration control



DPPE DOPE DOPA DPPC DOPC DPPG DOPG

B

Immunostaining



DPPE DOPE DOPA DPPC DOPC DPPG DOPG



# Supplementary data, Table S1

	<i>O. oeni</i> Exponential	<i>O. oeni</i> Stationary	<i>O. oeni</i> Ethanol 8%	<i>L. plantarum</i>	
Fatty acids (%)	<b>C14:0</b>	3.7 ± 0.5 A	3.5 ± 0.5 A	2.3 ± 0.4 AB	1.8 ± 0.2 B
	<b>C15:0</b>	0.6 ± 0.1 A	0.5 ± 0.1 A	0.8 ± 0.1 A	0.1 ± 0 B
	<b>C16:1</b>	2.4 ± 0.6 A	1.9 ± 0.5 A	0.8 ± 0.3 A	3.9 ± 0.8 B
	<b>C16:0</b>	36.9 ± 6.3 A	29.6 ± 3.1 A	42.2 ± 6.5 A	42.1 ± 5.1 A
	<b>C17:1</b>	0.6 ± 0.1 A	0.4 ± 0.1 AB	0.3 ± 0.1 BC	0.2 ± 0.1 C
	<b>C17:0</b>	0.4 ± 0.1 B	0.4 ± 0.1 B	0.7 ± 0.1 A	0.1 ± 0 C
	<b>C18:1</b>	26.3 ± 2 A	25.5 ± 1.1 A	11.5 ± 5.1 B	20 ± 0.7 B
	<b>C18:0</b>	7.9 ± 2.7 A	8.6 ± 2.3 A	21 ± 3.3 B	4.9 ± 0.3 A
	<b>C19:1</b>	21.2 ± 2.2 A	29.6 ± 1.9 A	20.4 ± 3.9 A	26.9 ± 4.2 A
Polar head groups (%)	<b>DGDG</b>	37.5 ± 33.5 AB	63.8 ± 5.3 A	56.7 ± 13.3 A	21.6 ± 0.9 B
	<b>MGDG</b>	22 ± 6.7 A	24.8 ± 3.2 A	18.7 ± 4.9 A	0.3 ± 0.1 B
	<b>DG</b>	1.7 ± 0.3 A	4.7 ± 1.3 A	3.7 ± 1.1 A	3.4 ± 0.7 A
	<b>Lysyl-PG</b>	0.2 ± 0.2 A	0 ± 0 A	0 ± 0 A	7.2 ± 1.1 B
	<b>PG</b>	38.6 ± 2.7 AB	6.7 ± 1.2 C	20.8 ± 10.9 BC	67.4 ± 2 A
	<b>CL</b>	0.009 ± 0.003 A	0.05 ± 0.01 B	0.02 ± 0.008 AB	0.002 ± 0.0005 C
	<b>PC</b>	0.0001 ± 0.00008 A	0.00006 ± 0.000004 A	0.0003 ± 0.0002 A	0.0007 ± 0.0001 B

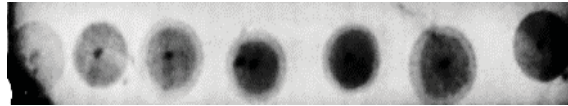
## Supplementary data, Table S2

		<i>O. oeni</i>			<i>L. plantarum</i>
Condition		Exponential	Stationary	Ethanol-adapted	Exponential
<b>Anisotropy without Lo18</b>	15°C	0.189	0.185	0.201	0.186
	65°C	0.070	0.105	0.108	0.070
	Rate of fluidification (%)	-63.0	-43.4	-46.2	-62.3
	Slope	-0.0024	-0.0016	-0.0019	-0.0023
<b>Anisotropy with Lo18</b>	15°C	0.220	0.228	0.239	0.208
	65°C	0.155	0.161	0.144	0.103
	Rate of fluidification (%)	-29.5	-29.2	-39.8	-50.5
	Slope	-0.0013	-0.0013	-0.0019	-0.0021

# Supplementary data, Figure S1

A

Nil Red coloration control



DPPE DOPE DOPA DPPC DOPC DPPG DOPG

B

Immunostaining



DPPE DOPE DOPA DPPC DOPC DPPG DOPG